Locking CNGA1 Channels in the Open and Closed State

Anil V. Nair, Monica Mazzolini, Paolo Codega, Alejandro Giorgetti, and Vincent Torre
International School for Advanced Studies and Instituto Nazionale Fisica della Materia, I-34014 Trieste, Italy

ABSTRACT With the aim of understanding the relation between structure and gating of CNGA1 channels from bovine rod, an extensive cysteine scanning mutagenesis was performed. Each residue from Phe-375 to Val-424 was mutated into a cysteine one at a time and the modification caused by various sulfhydryl reagents was analyzed. The addition of the mild oxidizing agent copper phenanthroline (CuP) in the open (presence of 1 mM cGMP) or closed state locked the channel in the respective states. A subsequent treatment with the reducing agent DTT restored normal gating fully in the open state and partially in the closed state. This action of CuP was not observed when F380 was mutated into a cysteine in the cysteine-free CNGA1 channel and in the double mutant C314S&F380C. These observations suggest that these effects are mediated by the formation of a disulfide bond (S-S) between F380C and the endogenous Cys-314 in the S5 segment. It can be rationalized by supposing that during gating the S6 segment rotates anticlockwise—when viewed from the extracellular side—by ~30°.

INTRODUCTION

CNG channels play a major role in sensory transduction of vertebrate photoreceptors and olfactory sensory neurons. They require cyclic nucleotides to open (1–7). Native CNG channels are heterotetramers composed of distinct subunit referred to as CNGA and CNGB (8,9). Homotetrameric CNGA1 channels from bovine rods when heterologously expressed give rise to functional channels with properties similar but not identical to those of native CNG channels (4). Each subunit is composed of 690 residues (4) encoding for a cyclic nucleotide-binding (CNB) domain made of ~125 amino acids in the cytoplasmic C-terminal end (5,7).

The amino acid sequences of CNG and K^+ channels have a significant homology and both channels are members of the superfamily of voltage-gated channels (5). Therefore, it is highly possible that CNG and K^+ channels share the same gross three-dimensional (3D) topology. The 3D structure of several K^+ channels has been solved recently: the bacterial KcsA from *Streptomyces lividans* in the closed state (10,11), the bacterial MthK from *Methanobacterium thermautotrophicum* in the open state (12,13), and the KirBac 1.1 in the closed state (14). In all these K^+ channels the pore domain includes four identical subunits comprising two transmembrane helices, S5 and S6 (referred to as TM1 and TM2 in KcsA and MthK channels), a loop forming the filter region, and an additional small helix, not spanning the lipid membrane referred to as the P-helix (Fig. 1). S6 is involved in the gating of K^+ channels, whereas the loop forming the filter region does not change its conformation upon gating. In K^+ channels, the major structural difference on passing from the closed to open conformation is the bending of S6 helix by 30° toward the lipid phase, around a glycine hinge (12,13).

In CNGA1 channels the gate is believed to be located in the pore itself (15–18) and a model of possible conformational changes in the pore region has been proposed (19). These conformational changes are initiated by the binding of cGMP in the CNB domain (4–7,18,20,21). This initial event must be transmitted to the pore region by conformational changes spanning throughout the entire cytoplasmic domain of the channel. As the S6 helix is connected to the C-linker and CNB domain, a signal must be transmitted to the pore region through S6.

With the aim of understanding the nature of this signal an extensive site-directed cysteine scanning mutagenesis was performed. Each residue—one by one—from Phe-375 to Val-424 was mutated into a cysteine and the modification produced by various sulfhydryl reagents was analyzed. During this analysis, we observed that mutant channel F380C was blocked by Cd^{2+} ions in the closed state but was potentiated in the open state. The irreversible potentiation of the mutant F380C caused by the addition of Cd^{2+} in the open state suggests some major changes in the gating of the mutant channel and we asked whether it was possible to lock the channel in the open state, in a way similar to that observed in the spHCN channel (22,23). Therefore we explored properties of the mutant channel F380C in more detail. The application of the mild oxidizing agent CuP in the presence of cGMP locked the channel in the open state. The addition of CuP in the closed state locked the channel in the closed state. The application of CuP did not lock the mutant channel F380C in a cysteine-free CNGA1 channel (24) neither in the open nor in the closed state. Similarly, application of CuP to the double mutant channel F380C&C314S did not have any significant effect. These results suggest the formation of disulfide bonds (S-S) between exogenous cysteines introduced in position 380 and endogenous Cys-314 in the S5 segment were responsible for the effect observed in the mutant channel F380C. These results provide clues for understanding

Submitted August 29, 2005, and accepted for publication February 3, 2006.

Address reprint requests to Vincent Torre, International School for Advanced Studies, Via Beirut 2-4, I-34014 Trieste, Italy. Tel.: 39-040-2240470; Fax: 39-040-2240470; E-mail: torre@sissa.it.

Alejandro Giorgetti's present address is Biocomputing Department of Biochemical Sciences, University of Rome ''La Sapienza'' P.le Aldo Moro, 5 00185 Rome, Italy.

0006-3495/06/05/3599/09 $2.00

doi: 10.1529/biophysj.105.073346

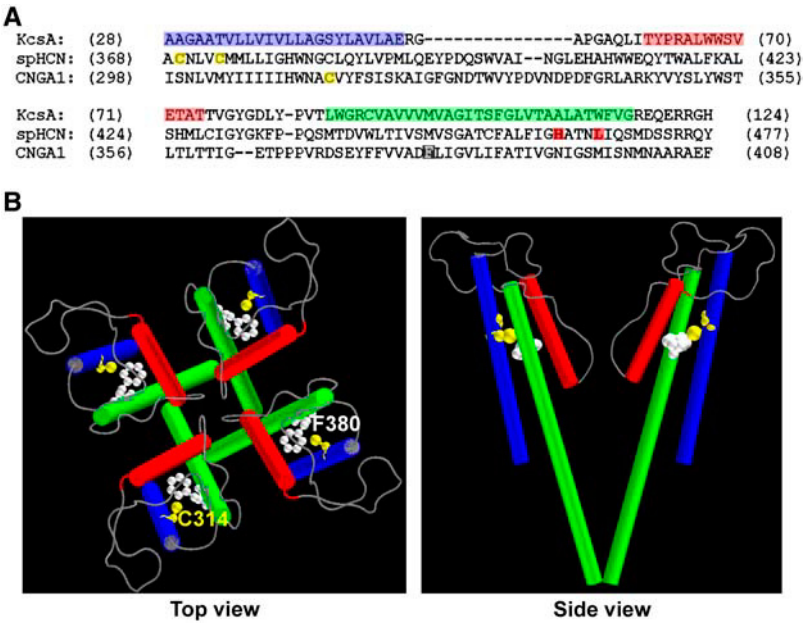

FIGURE 1 Sequence alignment of the KcsA, CNGA1, and spHCN channels. (*A*) Sequence alignments between the KcsA (K^+ channel from *Streptomyces lividans*), the CNGA1, and the spHCN channel (HCN channel from sea urchin sperm). Residues in blue, red, and green boxes of the KcsA channel indicate the S5, the P-helix, and the S6 domain, known to have an α-helical conformation. Yellow indicates cysteine residues. Residues involved in locking the spHCN channel in the open state (22) are shown in red boxes and Phe-380 of the CNGA1 channel is shown in a black box. (*B*) Homology model of CNGA1 channel showing the location of Cys-314 (in *yellow*) in the S5 domain flanking Phe-380 (in *white*) in the S6 domain. The homology model was obtained using the 3D structure of the KcsA channel as template with the sequence alignment shown in panel *A*. A top view of the homology model is shown on the left panel and a side view on the right. Colored cylinders indicate α-helices; blue, red, and green indicate the S5, the P-helix, and the S6 presumed domains.

conformational changes in the upper part of the S6 domain, which leads to channel opening (19).

MATERIALS AND METHODS

Molecular biology

The clone of the BROD CNGA1 channel, consisting of 690 residues, was mutated using the Quick Change Site-Directed Mutagenesis kit (Stratagene, La Jolla, CA). The DNA was sequenced with the sequencer LI-COR (4000L) to verify whether the mutation was correct. The selected residues were replaced by introducing a cysteine in the wild-type (WT) and cysteine-free WT as described (16,24). The double mutants were constructed by insertion of an additional mutation into the DNA with a single mutation. The RNAs were synthesized in vitro by using the mCAP RNA Capping kit (Stratagene).

Oocyte preparation and chemicals

The WT or mutant channel cRNAs were injected into *Xenopus laevis* oocytes (''Rettili'' Dr. Rainer Schneider, Varese, Italy). Oocytes were prepared as described (25). Injected eggs were maintained at 19°C in a Barth solution supplemented with 50 μg/ml gentamycin sulfate and containing (in mM): 88 NaCl, 1 KCl, 0.82 $MgSO_4$, 0.33 $Ca(NO_3)_2$, 0.41 $CaCl_2$, 2.4 $NaHCO_3$, 5 TRIS-HCl, pH 7.4 (buffered with NaOH). During the experiments, oocytes were kept in a Ringer solution containing (in mM): 150 NaCl, 2.5 KCl, 1 $CaCl_2$, 1.6 $MgCl_2$, 10 HEPES-NaOH, pH 7.4 (buffered with NaOH). All chemicals were purchased from Sigma Chemicals (St. Louis, MO).

Recording apparatus

cGMP-gated currents from excised patches were recorded with a patch-clamp amplifier (Axopatch 200B, Axon Instruments, Foster City, CA), 2–6 days after RNA injection, at room temperature (20–24°C). The perfusion system was as described (26) and allowed a complete solution change in $<$200 ms. Borosilicate glass pipettes had resistances of 3–5 MΩ in symmetrical standard solution. The standard solution on both sides of the membrane consisted of (in mM) NaCl, 110; HEPES, 10; and EDTA, 0.2 (pH 7.4). The membrane potential was usually stepped from 0 to $\pm$60 mV. We used Clampex 8.0, Clampfit, and Matlab for data acquisition and analysis. Currents were low-pass filtered at 2 kHz and acquired digitally at 5 kHz.

Application of sulfhydryl-specific reagents

In the inside-out patch-clamp configuration, soon after patch excision, the cytoplasmic face of the plasma membrane was perfused with the same pipette-filling solution and then with the same solution containing 1 mM cGMP. The Cd^{2+} effect was tested by perfusing the intracellular side of the membrane with a standard solution without EDTA (to avoid partial Cd^{2+} chelation), supplemented with 100 μM $CdCl_2$ for variable time course, to study the effect in the closed state. For the open state we applied the above solution in the presence of 1 mM cGMP. CuP was prepared by mixing cupric sulfate and phenanthroline in a 1:3 ratio to a final concentration of 1 (or 10) μM of $CuSO_4$ in the standard solution without EDTA. Phenanthroline was dissolved in ethanol and cupric sulfate in water. DTT (5 mM) was dissolved in the standard solution without EDTA. CuP and DTT was freshly prepared everyday. DTT was used for a maximum of 5 h. Current traces illustrated in the figures were obtained by subtracting the current measured in the absence of cGMP before application of CuP and DTT to the current measured after the ionic manipulations (addition and removal of CuP, DTT, or cGMP) of the intracellular medium. Therefore, the current measured at the beginning of the experiment in the absence of cGMP is shown as zero (see *straight line* in panels *A* of Figs. 4–8).

Sequence alignment

Sequence alignments were performed using ClustalW multiple alignment program (27). Three-dimensional models of the S5, the P-helix, and the S6 domain of CNGA1 were constructed using a homology modeling approach as implemented in the program Modeller 6.2 (28,29). The molecular models in Figs. 1and 9 are prepared with VMD 1.8.2. visualization software.

RESULTS

CNG and K^+ channels belong to the same superfamily of voltage-gated ionic channels (30) and are most likely to share the common molecular architecture. Therefore, the structure of KcsA (10,11) is a possible template for the 3D structure of the pore, S5, and S6 domains of CNG channels (18). Fig. 1 *A* illustrates the sequence alignment between residues from Ala-28 to His-124 of the KcsA channel and from Iso-298 to Phe-408 of the CNGA1 channel and Ala-368–Tyr-477 of

spHCN channels (the hyperpolarization and cyclic nucleotide controlled channels from sea urchin sperm (31)). The S5, S6 domains and the P-helix of the KcsA channel are indicated in Fig. 1 *A* and it is believed that the aligned amino acids of the CNGA1 and spHCN channels have an α-helical configuration with a similar orientation in space.

With the aim of understanding the relation between structure and gating in CNGA1 channels an extensive site-directed cysteine scanning mutagenesis was performed in the S6 and C-linker domain of the CNGA1 channel and the effect of 100 μM Cd^{2+} added to the intracellular side of the membrane patch was investigated.

The mutant and WT constructs were expressed in *Xenopus laevis* oocytes and studied with the patch-clamp method in the excised inside-out patch configuration. The effect of the addition of 100 μM Cd^{2+} on the WT CNGA1 channel is illustrated in Fig. 2, *A–C*. Brief voltage pulses from −100 to +100 mV in step of 20 mV were alternated, while changing the medium bathing the intracellular side of the membrane patch. When Cd^{2+} ions were added in the presence of 1 mM cGMP (Fig. 2 *B*), the cGMP-activated current (Fig. 2 *A*) was reduced in a voltage-dependent way, presumably by binding to Glu-363 in the pore region (26,32). At higher negative voltages (below −40 mV; see also Becchetti and Roncaglia (15)), 100 μM Cd^{2+} did not block but potentiated the cGMP-activated current. This potentiation is similar to that observed in the presence of Ni^{2+} ions, known to be mediated by His-420 in the C-linker (33–35). Blockage at positive voltages and potentiation at higher negative voltages caused by 100 μM Cd^{2+} in the WT CNGA1 channel were fully reversible when Cd^{2+} ions were removed from the bathing medium (Fig. 2 *C*). Similarly, exposures to 100 μM Cd^{2+} in the absence of cGMP did not cause any significant alteration of the cGMP-activated current measured after removing Cd^{2+} ions. The current voltage relation of the cGMP activated current in the presence of 1 mM cGMP and with (*open symbols*) and without 100 μM Cd^{2+} (*solid symbols*) are shown in panel *D*: Cd^{2+} ions potentiate the cGMP-activated current at negative voltages and block the current at positive voltages. Very similar results were obtained with a cysteine-free CNGA1 channel, here referred as $WT_{cys\text{-}free}$ kindly provided by William Zagotta (24). These observations provide a rationale to distinguish the action of Cd^{2+} ions mediated by the binding to exogenously introduced cysteines: significant changes of the cGMP-activated current (i.e., >20%), observed after exposure to 100 μM Cd^{2+} can be attributed to exogenously introduced cysteines.

During the cysteine scanning analysis of residues from Phe-375 to Val-424 the exposure of the intracellular side of the membrane to 100 μM Cd^{2+} ions for 5 min either had a negligible effect or blocked in an irreversible way the cGMP evoked current. The remarkable exception was mutant channel F380C; as shown in Fig. 2 *D*, when the mutant channel was exposed for 5 min to 100 μM Cd^{2+} ions in the presence of 1 mM cGMP, the cGMP-activated current was permanently activated by 37 ± 15% ($n = 7$) both at positive and negative voltages for at least 15 min after removal of Cd^{2+} ions from the intracellular medium. On the contrary, when Cd^{2+} ions were

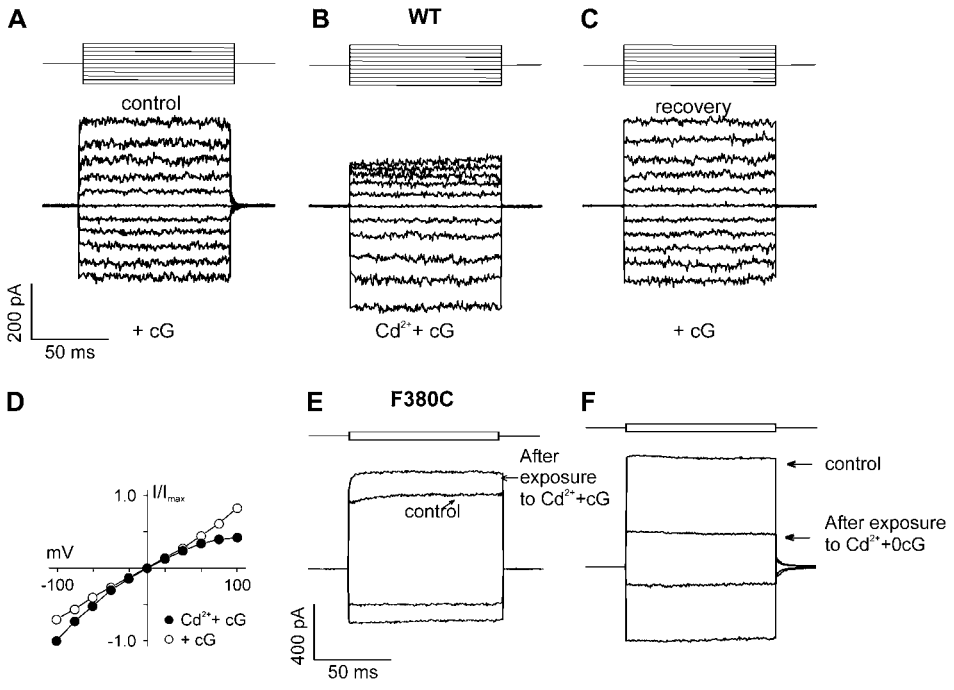

FIGURE 2 The effect of Cd^{2+} on the WT CNGA1 and mutant channel F380C. (*A–C*) Current recordings (average of three trials) at membrane voltages from −100 to 100 mV in 20 mV steps from the WT in control conditions (*A*), in the presence of 100 μM Cd^{2+} (*B*), and after removal of Cd^{2+} ions (*C*). No permanent modification in the cGMP-activated current after removal of Cd^{2+} ions was observed. (*D*) I/V relation of the WT. CNGA1 channel in control conditions (*open symbols*) and in the presence of 100 μM Cd^{2+} (*solid symbols*). (*E* and *F*) Permanent modification of the cGMP-activated current in mutant F380C after exposure to 100 μM Cd^{2+} ions in the presence and absence of 1 mM cGMP, respectively. In panels *D* and *E*, Cd^{2+} ions were applied for 5 min and the cGMP-activated current at ±60 mV was measured before application of Cd^{2+} ions (*traces labeled control*) and after removal of Cd^{2+} ions (*traces labeled after exposure* to Cd^{2+} + cG and Cd^{2+} + 0 cG) from the bathing solution. The cGMP-gated current was obtained as the difference of the current in the presence and in the absence of 1 mM cGMP. The current traces shown in panels *D* and *E* are the average of 10 individual trials. Thin horizontal lines represent the applied membrane potential.

added in the absence of cGMP, the cGMP-activated current was blocked both at positive and negative voltages for at least 15 min after Cd^{2+} removal (Fig. 2 *E*). Therefore we decided to investigate the mutant channel F380C in more detail.

Fig. 3 illustrates current recordings obtained from the WT (*A*), the mutant F380C (*B*), the $WT_{cys\text{-}free}$ (*C*), and the mutant channel $F380C_{cys\text{-}free}$ in a $WT_{cys\text{-}free}$ background (*D*), when the membrane voltage was applied from −100 to +100 mV in 20 mV steps. The mutant channel F380C either in the WT or in the $WT_{cys\text{-}free}$ background had a significant rectification: the ratio of the cGMP-activated current at −100 mV and at +100 mV in mutant channel F380C was 39 ± 19% ($n = 32$) and in the $WT_{cys\text{-}free}$ was 37 ± 22% ($n = 24$).

The irreversible potentiation of the mutant F380C (Fig. 2 *D*) caused by the addition of Cd^{2+} in the open state suggests some major changes in the gating of the mutant channel and we asked whether it was possible to lock the channel in the open state, in a way similar to that observed in the spHCN channel (22). Indeed, in the spHCN mutant channel L466C, nanomolar quantities of Cd^{2+} ions greatly slow down its closure once opened at negative voltages (22). In the presence of Cd^{2+} ions, the double mutant channel H462C&L466C once opened remains locked in the open configuration. This locking in the open state could be caused by the formation of disulfide bonds between exogenous cysteines and endogenous cysteines (Cys-373 and Cys-369 shown in *yellow* in Fig. 1 *A*) becoming close in the open state as suggested by Giorgetti et al. (23). Phe-380 (*white*) of the CNGA1 channel and His-462 and Leu-466 (*red*) of the spHCN channel are located in the S6 domain (Fig. 1 *A*), which presumably moves during channel gating. The yellow boxes in Fig. 1 *A* show the endogenous cysteines present in the S5 of the CNGA1 and spHCN channels. Fig. 1 *B* illustrates a top and side view of the molecular model of S5, pore, and S6 domains of the CNGA1 channel based on the homology with the KcsA channel and the sequence alignment of Fig. 1 *A*. According to this model, Cys-314 (shown in *yellow*) in the S5 domain is at a short distance from Phe-380 (shown in *white*) of the S6 domain. Therefore the endogenous Cys-314 could form S-S bonds with the exogenous sulfur atoms of mutant channel F380C. This interaction could be responsible for the locking of mutant channel F380C in the open and closed state, which will be described in the coming sections.

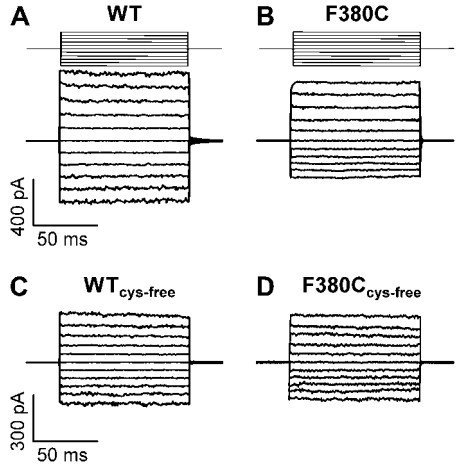

FIGURE 3 Comparison of the I/V relations in the WT (*A*), mutant F380C (*B*), $WT_{cys\text{-}free}$ (*C*), and mutant channel $F380C_{cys\text{-}free}$ in the $WT_{cys\text{-}free}$ background (*D*); current recordings at membrane voltages from −100 to 100 mV in 20 mV steps are shown. Each trace was obtained as an average of five individual trials. The cGMP-gated current was obtained as the difference of the current in the presence and in the absence of 1 mM cGMP. Thin horizontal lines represent the applied membrane potential.

Locking of mutant channel F380C in the open state

When mutant channel F380C in the presence of 1 mM cGMP was exposed to the mild oxidizing agent CuP (1 or 10 μM) for some tens of seconds the amplitude of the cGMP-activated current increased significantly. After an exposure for several minutes to CuP in the presence of 1 mM cGMP, the cGMP-activated current persisted even after cGMP was removed from the solution bathing the intracellular side of the patch (Fig. 4, *A* and *B*). After exposure to CuP (1 or 10 μM) in the presence of 1 mM cGMP for at least 3 min, the current measured in the absence of cGMP significantly increased: data collected from 26 patches indicate that the current measured in the absence of cGMP was 68 ± 25% of that measured in the presence of 1 mM cGMP before CuP with cGMP application. This behavior could be either due to the locking of the channel in the open state (locked open) or due to an increase in the leak current caused by the deterioration of the patch. Two reasons suggest that the channels were locked in the open state. Firstly, as shown in Fig. 4, *E* and *F*, the I/V relations of the current flowing through the patch after CuP treatment had the same degree of rectification as the cGMP-activated current before CuP treatment; indeed the ratio of the cGMP-activated current at −100 mV and at +100 mV in mutant channel F380C was 39 ± 19% ($n = 32$) before exposure to CuP and after treatment of CuP in the presence of 1 mM cGMP. The same ratio of currents of CuP treatment in the absence of cGMP was 35 ± 23% ($n = 15$). Secondly, 100 μM Cd^{2+} blocked the current measured in the absence of cGMP of locked-open channel (Fig. 4, *D* and *F*) with the same voltage-dependent way as the current measured in the presence of 1 mM cGMP before CuP application (Fig. 4, *C* and *E*); the current at positive voltage is blocked more powerfully than the current at negative voltages. In addition, as shown in Fig. 4, *C* and *D*, a clear potentiation of the cGMP-activated current at higher negative voltages was observed, as observed in the WT CNGA1 channel (see Fig. 2). The blocking effect of Cd^{2+} ions of the cGMP-activated current at positive voltages was significantly larger in the mutant F380C than in the WT channel (compare Figs. 2 and 4), as shown from the current voltage relations shown in Fig. 4, *E* and *F*.

Perfusing mutant channels F380C locked in the open state with the standard solution without cGMP for several minutes

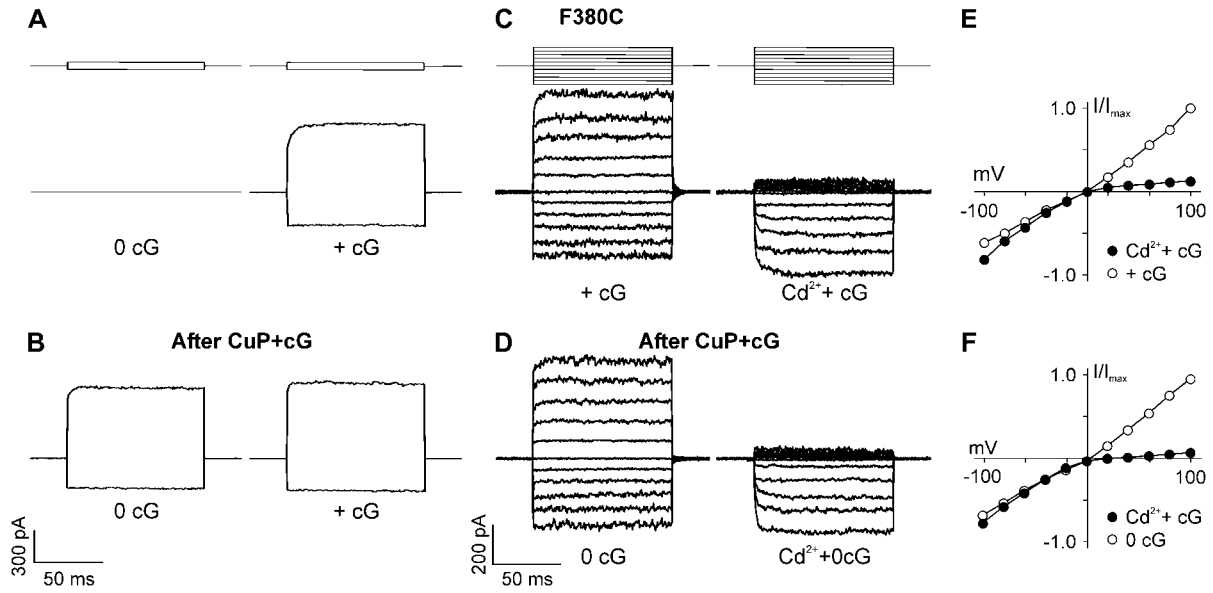

FIGURE 4 CuP in the presence of 1 mM cGMP locks the mutant channel F380C in the open state. (*A*) Currents recorded in the absence of cGMP (0 cG) and in the presence of 1 mM cGMP (+ cG) in mutant channels F380C. (*B*) The effect of exposure to 1 μM CuP for 5 min in the presence of 1 mM cGMP on the currents recorded in the absence of cGMP (0 cG) and in the presence of 1 mM cGMP (+ cG). In panels *A* and *B*, current recordings were obtained at $\pm$60 mV by averaging 10 individual trials. (*C*) The blockage of cGMP-activated current (+ cG) by 100 μM Cd^{2+} added to the medium bathing the intracellular side of the membrane patch (Cd^{2+} + cG) before CuP treatment. (*D*) Blockage by 100 μM Cd^{2+} (Cd^{2+} + 0 cG) of the current persistent (0 cG) in a locked-open channel after exposure to CuP + 1 mM cGMP. (*E*) I/V relation of the mutant F380C channel in control conditions (*open symbols*) and in the presence of 100 μM Cd^{2+} (*solid symbols*). (*F*) I/V relation of the current persistent in a locked-open channel (*open symbols*) and in the presence of 100 μM Cd^{2+} (*solid symbols*). In panels *A* and *C* the cGMP-activated current was obtained by subtracting the current measured in the absence of cGMP from the current measured in the presence of 1 mM cGMP. In panels *B* and *D* the current was obtained by subtracting the current measured in the absence of cGMP before CuP exposure from the current measured after CuP exposure. In panels *C* and *D* current recordings were obtained by averaging three individual trials each obtained at voltages from -100 to $+100$ mV in steps of 20 mV. Thin horizontal lines represent the applied membrane potential.

did not unlock mutant channels. The locking of the channel in the open state could be caused by the formation of disulfide bonds between the sulfur atoms of exogenous cysteines and endogenous cysteines (Fig. 1). In this case treatment with the reducing agent DTT is expected to break these disulfide bonds and unlock the channel from the open configuration. CuP could also overoxidize cysteines and this modification is not reverted by DTT (36).

After treatment with 5 mM DTT for 5 min the amplitude of the current recorded in the absence of cGMP (Fig. 5 *B*) in the locked-open mutant channel F380C decreased and approached the amplitude of current observed before CuP treatment (*gray trace* in Fig. 5 *A*). The amplitude of the current observed in the presence of cGMP was almost unaffected by treatment with DTT (compare Fig. 5, *A* and *B*). Collected data from six patches showed that DTT reduced the current measured in the absence of cGMP in the locked-open channel by 70 $\pm$ 25%.

Locking of mutant channel F380C in the closed state

Next we addressed the question: what would happen if mutant channels F380C were treated with CuP in the absence of cGMP? When the patch was treated with CuP in the closed state—i.e., in the absence of cGMP—the cGMP-activated current (Fig. 6 *A*) was abolished, as shown in Fig. 6 *B*. Indeed the current measured in the presence and absence of cGMP did not show any rectification and had amplitude similar to

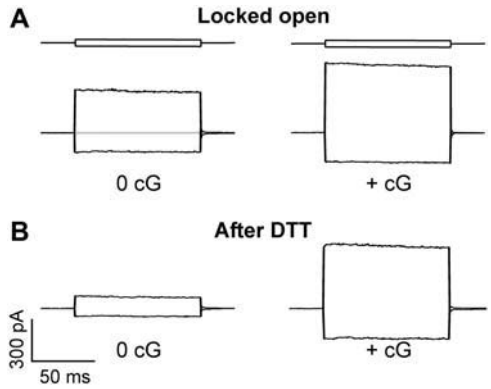

FIGURE 5 The locking of mutant F380C in the open state is reverted by DTT. (*A*) The current measured in the absence (0 cG) and in the presence of 1 mM cGMP (+ cG) after exposure to CuP in the presence of 1 mM cGMP for 5 min. The gray trace in the first column indicates the current measured under the same conditions before CuP exposure. (*B*) Same as in panel *A*, but after removal of CuP and exposure to 5 mM DTT for 5 min in the absence of cGMP. Current traces shown are obtained as in Fig. 4 *B*. Thin horizontal lines represent the applied membrane potential.

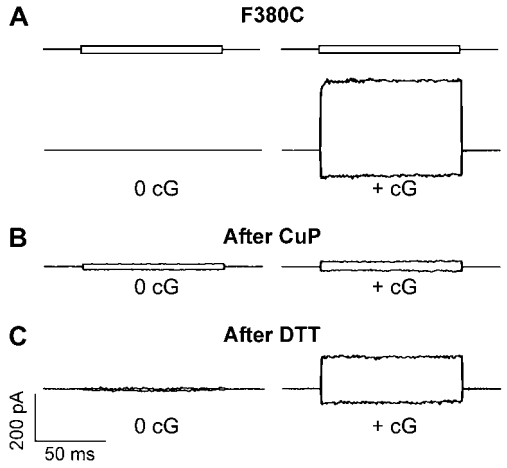

FIGURE 6 Locking of mutant channel F380C by CuP in the absence of cGMP. (*A*) Currents recorded in the absence of cGMP (0 cG) and in the presence of 1 mM cGMP (+ cG) before CuP exposure. (*B*) Same as in panel *A* but after exposure to 1 μM CuP for 5 min in the absence of cGMP. (*C*) Same as in panel *B* but after removal of CuP and exposure to 5 mM DTT in the absence of cGMP for 5 min. Current traces shown are obtained as in Fig. 4 *B*. Thin horizontal lines represent the applied membrane potential.

that observed in the absence of cGMP before CuP treatment. In all 19 patches examined, the exposure to CuP in the absence of cGMP for longer than 5 min invariably led to an almost complete blockage of the cGMP-activated current (locked closed). When mutant channels F380C were locked in the closed state by treatment with CuP (Fig. 6 *B*), a subsequent treatment with DTT unlocked (Fig. 6 *C*) these channels to some extent. DTT treatment (5 mM) for 5 min restored 46 $\pm$ 24% (six patches) of the current initially observed in the presence of 1 mM cGMP before CuP treatment.

Mutant channel F380C in a cysteine-free background and the double mutant channel F380C&C314S

The homology modeling of Fig. 1 *B* suggest that the exogenous cysteines introduced in the position 380 are far apart to form intersubunit disulfide bonds. To investigate the possible formation of disulfide bonds between endogenous and exogenous cysteines, we repeated the mutation F380C in a cysteine-free CNGA1 channel ($F380C_{cys\text{-}free}$) kindly provided by Matulef et al. (24). Data obtained from different patches show that treatment with CuP for 5 min in the open (seven patches) or closed (six patches) state did not lock the channel in either states (Fig. 7, *A* and *B*).

Sequence alignment of the CNGA1 and KcsA channel (Fig. 1 *A*) and the homology model with the 3D structure of the KcsA channel (Fig. 1 *B*) show that in the S5 domain of CNGA1 there is a native cysteine at position 314 that could form a disulfide bond with the exogenous cysteine at position 380, responsible for the effects described in Figs. 4–6. To test this possibility the mutant channel F380C&C314S was constructed. Incubation of patch in CuP for 5 min in the presence

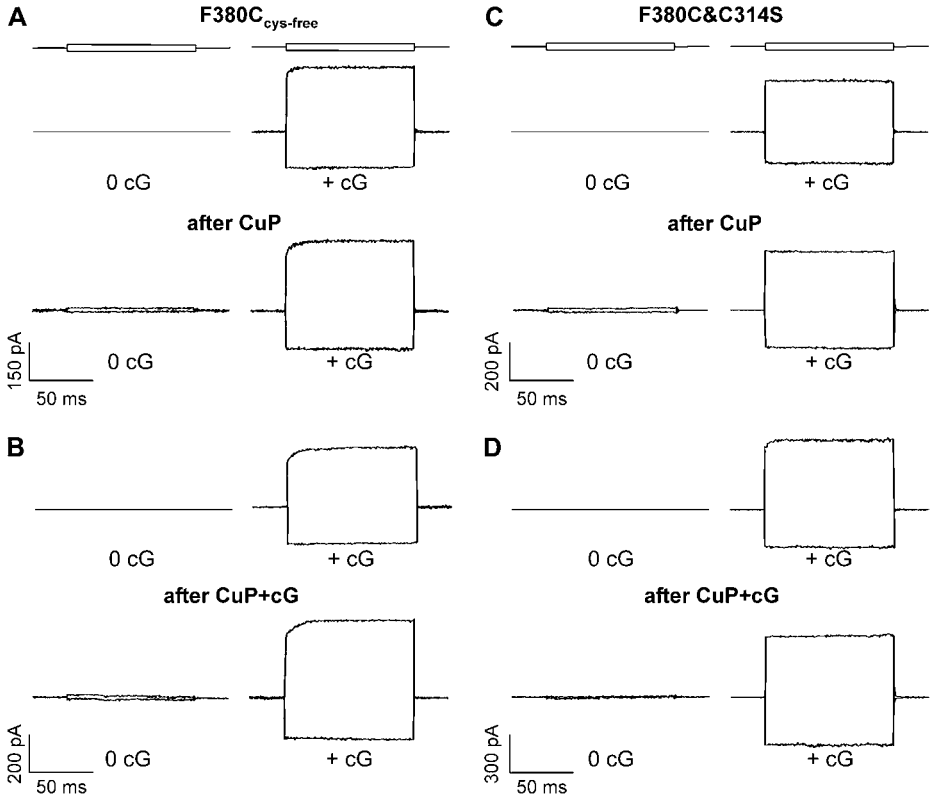

FIGURE 7 CuP has no effect on the mutants $F380C_{cys\text{-}free}$ and double mutant F380C&C314S. (*A* and *B*) The effect of exposure to 1 μM CuP for 5 min in the absence of cGMP (*A*) and in its presence (*B*) on the mutant F380C in the cysteine-free WT ($F380C_{cys\text{-}free}$). (*C* and *D*) The effect of the exposure for 5 min to 1 μM CuP in the absence of 1 mM cGMP (*C*) and in its presence (*D*) on the double mutant F380C&C314S. 0 cG represents the current measured in the absence of cGMP and + cG represents the current measured in the presence of 1 mM cGMP. Current traces shown are obtained as in Fig. 4 *B*. Thin horizontal lines represent the applied membrane potential.

or in the absence of cGMP did not lock the channel in both conformations (Fig. 7, *C* and *D*). Similar results were observed in four different patches excised from two different oocytes.

To verify whether the locking of the channel in the open and closed state described in Figs. 3–6 was caused primarily and uniquely by the formation of disulfide bonds between cysteines in positions 380 and 314, cysteines were introduced at positions 380 and 314 in the cysteine-free CNGA1 background. CuP was able to lock—to some extent—also this mutant channel (Fig. 8, *A* and *B*) in the closed and open state as observed in the mutant F380C. After CuP application in the closed state the cGMP-activated current was reduced by 49 ± 23% ($n = 7$). After application of CuP in the presence of 1 mM cGMP the current measured in the absence of cGMP was 51 ± 28% ($n = 6$) of the current measured in the presence of cGMP. Therefore the effect of CuP on the mutant F380C is similar but not identical to that observed on the mutant F380C&C314$_{\text{cys-free}}$ constructed on the WT$_{\text{cys-free}}$ background.

All these results show that the mechanism responsible for locking the channel in the open and closed state is indeed due to the formation of disulfide bonds between cysteines in positions 380 and 314.

DISCUSSION

Upon binding of cyclic nucleotide, CNG channels undergo a sequence of conformational changes leading to channel opening (1). As the binding domain is located in the cytoplasm (4) and the gate is presumably located in the pore itself (15–18) a signal must be transmitted to the S6 domain and finally to the pore. The nature of this signal is unknown and constitutes the molecular basis of channel gating. Locking CNG channels in the open and closed state provides useful information on conformational changes that occur during gating. Our results show that in mutant channel F380C, the addition of the oxidizing agent CuP in the open and closed state locks CNGA1 channels in the respective states. Moreover DTT, a reducing agent, unlocks the channels from their locked configuration. These results suggest that the observed locking effect was mediated by the formation of disulfide bridges. When a cysteine at position 380 was introduced in the cysteine-free CNGA1 wild-type channel (24) CuP could not lock the channel in either state. Also in the double mutant F380C&C314S CuP could not lock the channel in open or closed states. Two cysteines were introduced at positions 380 and 314 in the cysteine-free CNGA1 background for the conformation of this observation. CuP was able to lock—to some extent—also this mutant channel (Fig. 8, *A* and *B*) in the closed and open state. These results indicate the formation of disulfide bridges between the exogenous cysteine introduced at position 380 and the endogenous cysteine at position 314.

These experimental observations can be used to hypothesize the signal originating from the cyclic nucleotide-binding domain and sent to the pore through the S6 domain. As suggested by our experiments Cys-314 of S5 and the exogenous cysteine in position 380 are near each other, both in the open and closed state so that in both states they can form a disulfide bond. Inspection of the Protein Data Bank (PDB) indicates that the distance between the C_α of cysteines forming a S-S bond is between 6 and 9 Å. Therefore, the distance between the C_α of the exogenous cysteine of mutant F380C and the endogenous Cys-314 must be within this range in both states. As a consequence, the conformational rearrangement that occurs during gating in the upper part of S6—where Phe-380 is located—does not involve large molecular motions but a subtle displacement; likely just a few Angstroms are enough to lead a major functional change.

A possible motion compatible with these experimental constraints is a rotation of the S6 domain around its helical axis by ~30° (Fig. 9). In the closed state the F380C and Cys-314 of each subunit can form an S-S bond, locking the channel in the closed state, as illustrated in Fig. 9.

In the open state (Fig. 9) the upper portion of S6 rotates anticlockwise by ~30°, when viewed from the extracellular side. Also in this configuration F380C and Cys-314 can form

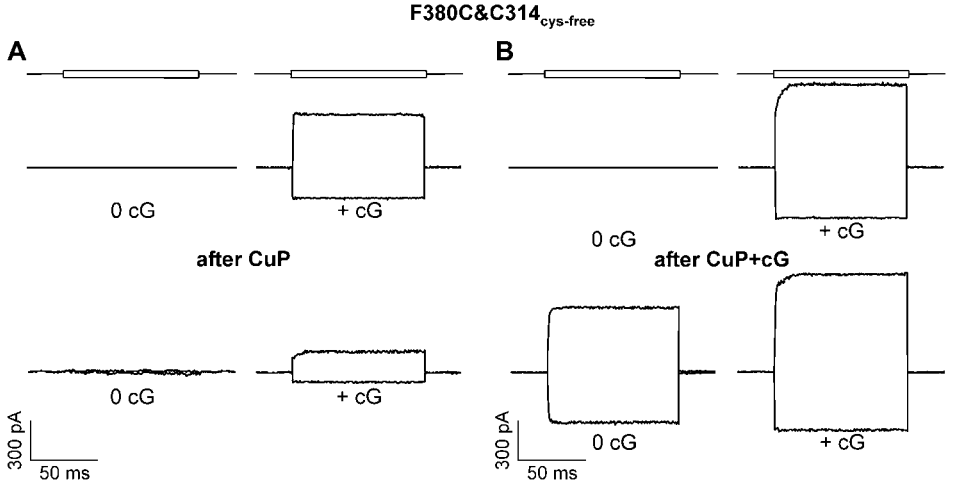

FIGURE 8 The effect of CuP in the absence and in the presence of 1 mM cGMP on the mutant channel F380C&C314$_{\text{cys-free}}$ constructed in the WT$_{\text{cys-free}}$ background. (*A* and *B*) Same as in Fig. 7, *A* and *B*. Current traces obtained as in Fig. 7. Thin horizontal lines represent the applied membrane potential.

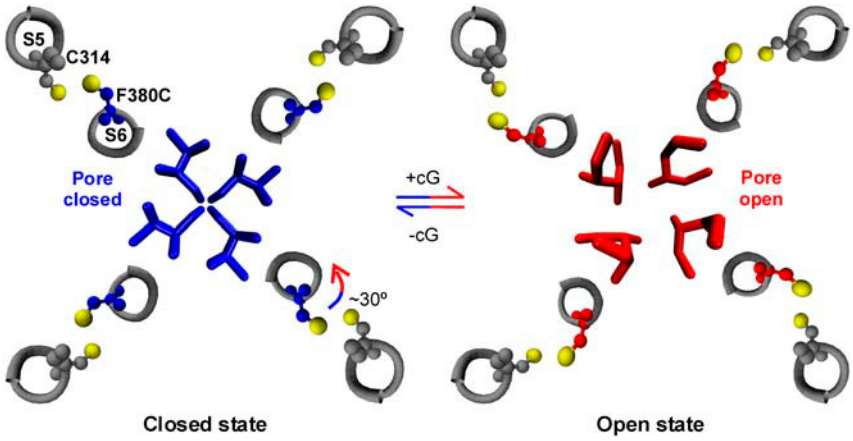

FIGURE 9 A model of the conformational changes during gating in the upper portion of S6 and the locking of mutant channel F380C in the closed and open state. Locking is mediated by the formation of disulfide bonds between the exogenous cysteines of mutant F380C and the endogenous cysteine Cys-314. The blue and red residues in the center show the narrowest region of the pore in the closed state and open state, respectively. In the open state the upper portion of S6 rotates anticlockwise—when viewed from the extracellular side of the membrane—by ~30°. This anticlockwise rotation, by a suitable coupling between the P-helix and S6 causes a small displacement of residues forming the narrowest portion of the pore leading to channel opening (see *red* residues). The position of the F380 has been slightly displaced from the analogous position of the corresponding residue (Met-96) of the KcsA structure (11), which points toward the selectivity filter.

an S-S bond but this time locking the channel in the open configuration. This anticlockwise rotation, by a suitable coupling between the P-helix and S6 causes a small displacement of residues that are forming the narrowest portion of the pore, leading to channel opening as hypothesized and shown in Fig. 9. The notion that channel gating is mediated by an anticlockwise rotation of the S6 domain was already proposed (37) on the basis of a histidine scanning of the S6 domain. An anticlockwise rotation of ~30° of the upper portion of S6 (19) may be the molecular signal underlying gating in the pore of CNGA1 channels. In this view we speculate that in the WT CNGA1 channel Phe-380 by interacting also with hydrophobic residues such as those comprised between Leu-351 and Leu-356 in the P-helix is part of the molecular coupling between the P-helix and S6.

The model described in Fig. 9 providing a molecular explanation of the locking of the channel in the open and closed state is certainly not unique and other mechanisms could be envisaged. For instance it is possible that in the closed state, blockage is mediated by the formation of disulfide bonds between cysteines within the same subunit and in the open state by the formation of disulfide bonds between cysteines in neighboring subunits or vice versa. This mechanism, however, requires large conformational changes of the pore topology between the open and closed state, which do not appear to be supported by the available experimental evidence. The fact that the mutant channels F380C&C314S and F380C$_{cys\text{-}free}$ did not lock the channels in either states by the application of CuP also strengthens the current notion. Indeed, the pattern of accessibility of residues in the pore region are very similar in the open and closed states (16,17) indicating that only minor and subtle conformational changes of the pore mediate the transition between the open and closed state. The model in Fig. 9 is certainly consistent with the experimental results described in this article and requires only small conformational changes for gating. The results obtained from different laboratories also support this model.

We thank William Zagotta who generously supplied us with the DNA of the WT and cysteine-free WT of BROD CNGA1 channel, and Claudio Anselmi for the helpful discussions.

This work was supported by a Human Frontier Science Program grant (RGP005A/2002 to V.T.), a COFIN grant from the Italian Ministry, a grant from CIPE (GRAND FVG), and the FIRB project RBLA03AF28 of the Italian Ministry of Research (MIUR).

REFERENCES

1. Fesenko, E. E., S. S. Kolesnikov, and A. L. Lyubarsky. 1985. Induction by cyclic GMP of cationic conductance in plasma membrane of retinal rod outer segment. *Nature*. 313:310–313.
2. Zimmerman, A. L., G. Yamanaka, F. Eckstein, D. A. Baylor, and L. Stryer. 1985. Interaction of hydrolysis-resistant analogs of cyclic GMP with the phosphodiesterase and light-sensitive channel of retinal rod outer segments. *Proc. Natl. Acad. Sci. USA*. 82:8813–8817.
3. Nakamura, T., and G. H. Gold. 1987. A cyclic nucleotide-gated conductance in olfactory receptor cilia. *Nature*. 325:442–444.
4. Kaupp, U. B., T. Niidome, T. Tanabe, S. Terada, W. Bönigk, W. Stühmer, N. J. Cook, K. Kangawa, H. Matsuo, T. Hirose, T. Miyata, and S. Numa. 1989. Primary structure and functional expression from complementary DNA of the rod photoreceptor cyclic GMP-gated channel. *Nature*. 342:762–766.
5. Zagotta, W. N., and S. A. Siegelbaum. 1996. Structure and function of cyclic nucleotide-gated channels. *Annu. Rev. Neurosci.* 19:235–263.
6. Biel, M., X. Zong, F. A. Ludwing, A. Sautter, and F. Hofmann. 1999. Structure and function of cyclic nucleotide-gated channels. *Rev. Physiol. Biochem. Pharmacol.* 135:151–171.
7. Kaupp, U. B., and R. Seifert. 2002. Cyclic nucleotide gated channels. *Physiol. Rev.* 82:769–824.
8. Shammat, I. M., and S. E. Gordon. 1999. Stoichiometry and arrangement of subunits in rod cyclic nucleotide-gated channels. *Neuron*. 23:809–819.
9. He, Y., M. Ruiz, and J. W. Karpen. 2000. Constraining the subunit order of rod cyclic nucleotide-gated channels reveals a diagonal arrangement of like subunits. *Proc. Natl. Acad. Sci. USA*. 97:895–900.
10. Doyle, D. A., J. M. Cabral, R. A. Pfuetzner, A. Kuo, J. M. Gulbis, S. L. Cohen, B. T. Chait, and R. MacKinnon. 1998. The structure of the potassium channel: molecular basis of K^+ conduction and selectivity. *Science*. 280:69–77.
11. Zhou, Y., J. H. Morais-Cabral, A. Kaufman, and R. MacKinnon. 2001. Chemistry of ion coordination and hydration revealed by a K^+ channel-Fab complex at 2.0 Å resolution. *Nature*. 414:43–48.

12. Jiang, Y., A. Lee, J. Chen, M. Cadene, B. T. Chait, and R. MacKinnon. 2002. Crystal structure and mechanism of calcium gated potassium channel. *Nature*. 417:515–522.

13. Jiang, Y., A. Lee, J. Chen, M. Cadene, B. T. Chait, and R. MacKinnon. 2002. The open pore conformation of potassium channels. *Nature*. 417: 523–526.

14. Kuo, A., J. M. Gulbis, J. Antcliff, T. Rahman, E. Lowe, J. Zimmer, J. Cuthbertson, F. M. Ashcroft, T. Ezaki, and D. A. Doyle. 2003. Crystal structure of the potassium channel KirBac1.1 in the closed state. *Science*. 3000:1922–1926.

15. Becchetti, A., and P. Roncaglia. 2000. Cyclic nucleotide-gated channels: intra- and extracellular accessibility to Cd^{2+} of substituted cysteine residues within the P-loop. *Pflugers Arch*. 440:556–565.

16. Becchetti, A., K. Gamel, and V. Torre. 1999. Cyclic nucleotide-gated channels pore topology studied through the accessibility of reporter cysteines. *J. Gen. Physiol.* 114:377–392.

17. Liu, J., and S. A. Siegelbaum. 2000. Change of pore helix conformational state upon opening of cyclic nucleotide gated channels. *Neuron*. 28:899–909.

18. Flynn, G. E., and W. N. Zagotta. 2003. A cysteine scan of the inner vestibule of cyclic nucleotide gated channels reveals architecture and rearrangement of the pore. *J. Gen. Physiol.* 121:563–582.

19. Giorgetti, A., A. V. Nair, P. Codega, V. Torre, and P. Carloni. 2005. Structural basis of gating of CNG channels. *FEBS Lett.* 579:1968–1972.

20. Flynn, G. E., and W. N. Zagotta. 2001. Conformational changes in s6 coupled to the opening of cyclic neucleotide-gated channels. *Neuron*. 30:689–698.

21. Mazzolini, M., M. Punta, and V. Torre. 2002. Movement of the C-helix during the gating of cyclic nucleotide gated channels. *Biophys. J*. 83:3283–3295.

22. Rothberg, B., K. Shin, and G. Yellen. 2003. Movements near the gate of a hyperpolarization-activated cation channel. *J. Gen. Physiol.* 122: 501–510.

23. Giorgetti, A., P. Carloni, P. Mistrik, and V. Torre. 2005. A homology model of the pore region of HCN channels. *Biophys. J*. 89:932–944.

24. Matulef, K., G. E. Flynn, and W. N. Zagotta. 1999. Molecular rearrangements in the ligand-binding domain of cyclic nucleotide-gated channels. *Neuron*. 24:443–452.

25. Nizzari, M., F. Sesti, M. T. Giraudo, C. Virginio, A. Cattaneo, and V. Torre. 1993. Single-channel properties of cloned cGMP-activated channels from retinal rods. *Proc. Biol. Sci*. 254:69–74.

26. Sesti, F., E. Eismann, U. B. Kaupp, M. Nizzari, and V. Torre. 1995. The multi-ion nature of the cGMP-gated channel from vertebrate rods. *J. Physiol.* (*Lond.*). 487:17–36.

27. Thompson, J. D., D. G. Higgins, and T. J. Gibson. 1994. CLUSTAL W: improving the sensitivity of progressive multiple sequence alignment through sequence weighting, position-specific gap penalties and weight matrix choice. *Nucleic Acids Res.* 22:4673–4680.

28. Šali, A., and T. L. Blundell. 1993. Comparative protein modeling by satisfaction of spatial restraints. *J. Mol. Biol.* 234:779–815.

29. Sánchez, R., and A. Šali. 1997. Advances in comparative protein-structure modeling. *Curr. Opin. Struct. Biol.* 7:206–214.

30. Jan, L. Y., and Y. N. Jan. 1990. A superfamily of ion channels. *Nature*. 345:672.

31. Gauss, R., R. Seifert, and U. B. Kaupp. 1998. Molecular identification of a hyperpolarization-activated channel in sea urchin sperm. *Nature*. 393:583–587.

32. Root, M. J., and R. MacKinnon. 1993. Identification of an external divalent binding site in the pore of a cGMP-activated channel. *Neuron*. 11:459–466.

33. Gordon, S. E., and W. N. Zagotta. 1995. A histidine residue associated with the gate of the cyclic nucleotide-activated channels in rod photoreceptors. *Neuron*. 14:177–183.

34. Gordon, S. E., and W. N. Zagotta. 1995. Localization of regions affecting an allosteric transition in cyclic nucleotide-activated channels. *Neuron*. 14:857–864.

35. Gordon, S. E., and W. N. Zagotta. 1995. Subunit interactions in coordination of Ni^{2+} in cyclic nucleotide-gated channels. *Proc. Natl. Acad. Sci. USA*. 92:10222–10226.

36. Hua, L., and S. E. Gordon. 2005. Functional interaction between A′ helices in the C-linker of open CNG channels. *J. Gen. Physiol.* 125: 335–344.

37. Johnson, J. P., and W. N. Zagotta. 2001. Rotational movement during cyclic nucleotide-gated channel opening. *Nature*. 412: 917–921.